# A MICRO-STRUCTURAL APPROACH TO SNOW METAMORPHISM: Computed Tomography Experiments and Numerical Simulations

Thomas U. Kaempfer*
Cold Regions Research and Engineering Laboratory, Hanover, USA

Martin Schneebeli, Bernd Pinzer
WSL Swiss Federal Institute for Snow and Avalanche Research SLF, Davos, Switzerland

ABSTRACT: Snow on the ground is a porous material consisting of sintering ice grains and air filled pore space. Snow undergoes metamorphism, where mass fluxes change the snow micro-structure and as a consequence the physical properties of snow. Understanding snow metamorphism and the impact on physical properties is crucial in snow science. We studied metamorphosing snow under temperature gradients (TG) non-destructively using computed micro-tomography. We could observe the growth and sublimation of snow crystals within a snow pack in real-time. We developed a numerical heat and mass-transfer model for snow operating at the same length-scales and using tomography data from natural snow as geometrical input. The model uses a diffuse interface technique to handle the complex and evolving ice-matrix geometry. We studied the interplay between micro-structure, heat flow, sublimation-condensation, and mass transport using the numerical model together with the experiments. Locally, very high temperature and concentration gradients may occur, leading to large local fluxes and strong dynamics, while globally no flux enhancement could be observed. Growth and sublimation rates of individual crystals may differ significantly from the global mass flow through the snow and individual snow grains survive only short times within TG-metamorphosing snow. These observations require an integrated porous media approach compared to a destructive grain based view.

KEYWORDS: Snow, Metamorphism, Micro-Tomography, Numerical Modeling

## 1. INTRODUCTION

Snow is a porous material consisting of ice grains that are connected by bonds, air filled pore space, small amounts of impurities, and sometimes liquid water. The complex micro-structure of this material changes with time due to sintering processes and in particular the redistribution of matter by sublimation, re-sublimation, and diffusion of water vapor through the pore space. If snow is subjected to a temperature gradient, a water vapor concentration gradient in the pore space is induced. This leads to enhanced water vapor diffusion along the gradient and thus to a more rapid evolution of the snow micro-structure. This process is known as temperature gradient (TG) snow metamorphism.

* *Corresponding author address:* Thomas U. Kaempfer, PhD, U.S. Army Engineer Research and Development Center, Cold Regions Research and Engineering Laboratory, Hanover, NH 03755, USA, tel: 1 603 646 44 72, e-mail: thomas.kaempfer@usace.army.mil

Reciprocally, the snow micro-structure strongly influences the snow pack properties including mechanical, chemical, and thermo-physical properties. The strong link between snow micro-structure and physical properties was recognized early on and work on snow metamorphism is vast. We refer to Arons and Colbeck (1995) for a review. The most modern observational techniques are based on computed X-ray micro-tomography, $\mu$-CT (Brzoska *et al.*, 1999; Kaempfer *et al.*, 2005; Kerbrat *et al.*, 2008; Schneebeli and Sokratov, 2004) and allow for non-destructive observations of metamorphosing snow at a resolution of approximately 10 $\mu$m. On the modeling side, Flin *et al.* (2003) developed simulations of curvature driven metamorphism using $\mu$-CT data as input. Recently, Kaempfer and Plapp (2007; 2008) presented a more general phase-field approach to model snow metamorphism that also assimilates $\mu$-CT images as geometrical input. Experiments and numerical models that operate at the same micro-structural length scale are thus available. The purpose of this work is to show how their combination can be used to gain more insight into snow metamorphism processes.

## 2. COMPUTED MICRO-TOMOGRAPHY

We used a table-top X-ray micro-computer-tomograph (Scanco $\mu$CT80) to image metamorphosing snow (Schneebeli and Sokratov, 2004). The instrument is installed inside a cold-room and equipped with a specially designed snow-breeder that accommodates a 4.8 cm diameter and 2 cm high snow sample (Fig. 1). The sample can actively be heated at the bottom and is passively cooled to the cold-room temperature at the top, while it is strongly insulated on the side-walls to ensure a nearly mono-dimensional heat flow. Two heat flux sensors placed at the top and bottom measure the heat flow through the sample under the imposed temperature gradient.

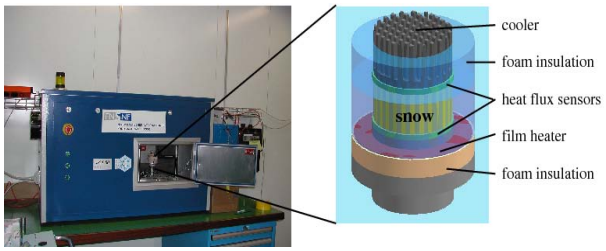


Figure 1: X-ray micro-tomograph ($\mu$-CT) with snow breeder.

We prepared two snow samples by sieving natural snow into the breeder. The snow consisted of small rounded grains at the beginning of the experiments and we determined its initial density by weighting to be 270 and 311 kg m$^{-3}$ for samples 1 and 2, respectively.

We subjected the snow to a constant temperature gradient, $\nabla T$, by keeping the mean temperature, T, constant with (T = -8.1 °C, $\nabla T$ = 46 K m$^{-1}$) for sample 1 and (T = -3.4 °C, $\nabla T$ = 49 K m$^{-1}$) for sample 2.

Periodically and for up to three weeks, we imaged the center of the snow cylinder at the same position by $\mu$-CT with a resolution of 25 $\mu$m (sample 1) or 18 $\mu$m (sample 2). The $\mu$-CT images were filtered with a Gaussian and median filter to reduce noise and segmented to create a binary 3D representation of the snow micro-structure consisting of the ice-matrix and the pore space. The segmentation threshold was chosen so that the initial weighted density was reproduced.

Due to the non-destructiveness of the method and because the samples were kept inside the $\mu$-CT and imaged at the exact same location, we could observe crystal growth and sublimation inside the snow during metamorphism. For example, inside sample 2, a large cup-crystal grows towards the warmer bottom of the sample, while it sublimates away at its top later (Fig. 2). It took approximately 2.5 days for a 0.7 mm large cup-crystal to form (see also section 4).

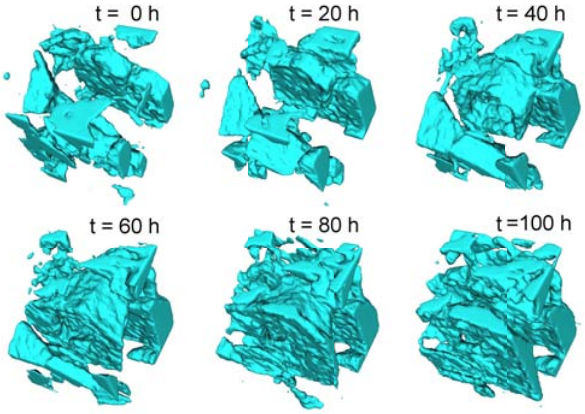


Figure 2: Growth of a cup-crystal within sample 2. The shown cube has 1.5 mm side-length.

By taking difference images of successive $\mu$-CT scans, we can determine the regions of crystal growth and sublimation (Fig. 3). In general, the growth proceeds against the water vapor flow that is induced by the temperature gradient from the warm (bottom) to the cold (top) of the samples. However, strong inhomogeneities can be observed.

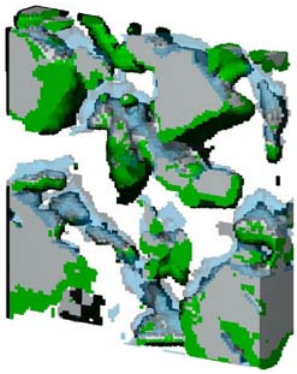

Figure 3: Difference image of two successive $\mu$-CT images of sample 1 taken one day apart and showing sublimated (blue) and condensed (green) ice. The shown domain is 2.5×0.375×2.5 mm.

We also use $\mu$-CT difference images to quantify mass flow during metamorphism by particle image velocimetry (section 4).

## 3. NUMERICAL METAMORPHISM MODEL

A detailed presentation of the numerical model (Kaempfer and Plapp, 2007; 2008) is out of scope for the present work and we restrict this section to a short discussion and results.

Snow metamorphism under an imposed temperature gradient is governed by heat and mass conservation laws, with phase change at ice-air interfaces. At these interfaces, capillary and kinetic effects influence sublimation and crystal growth. Large geometrical evolutions imply that numerical two-phase formulations with adaptive meshing (Christon *et al.,* 1994) are inefficient.

The phase field method is widely used to model the formation of complex micro-structures during solidification processes (Boettinger *et al.,* 2002) and is also ideally suited to model snow metamorphism at the scale of $\mu$-CT experiments. In fact, as a diffuse interface method it treats the problem continuously, inclusive of the ice-air interface region. The continuous variation across the interface is realized using an order parameter, the phase field function $\phi$, which describes the phases thermodynamically (Fig. 4).

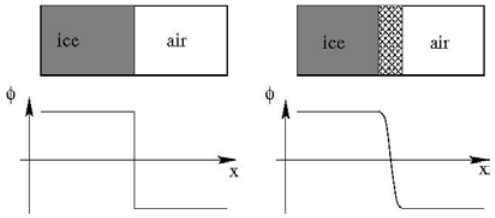


Figure 4: Sharp interface (left) and diffuse interface (right) with the phase field function $\phi$.

The basic diffusion equations, with supplementary phase field terms, are then deduced from a free energy functional $F(\phi)$ for the whole system and interface conditions do not occur but are replaced by a partial differential equation for $\phi$. Topological changes and capillary and kinetic effects are modeled implicitly through the definition of $F(\phi)$.

For the TG metamorphism problem, the phase-field driving force is related to the water vapor saturation in the pore space. That is, ice sublimates in regions of undersaturation and crystals grow where the pore space is supersaturated. The saturation pressure itself is determined in function of the local temperature, thus coupling heat and mass diffusion to the phase-field. For simplicity, we suppose that capillary and kinetic effects are isotropic.

Starting from a $\mu$-CT image of snow, we first define the phase-field $\phi$ by diffusing the ice-air interfaces (Fig. 5).

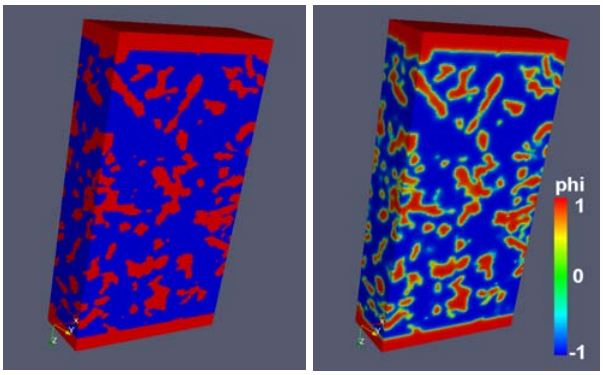


Figure 5: From a $\mu$-CT image (left) to the diffuse interface domain (right). The shown domain is 1.0×2.5×5.2 mm.

As in the experiments, we then impose temperatures at the bottom (warm) and top (cold) and compute the evolution of temperature, water vapor field in the pore space, and phase-change by solving iteratively the time-dependent heat and mass diffusion equations, together with the phase-field equation (Fig. 6). Regions of grain growth and sublimation correspond well to the experimental difference images (Fig. 3).

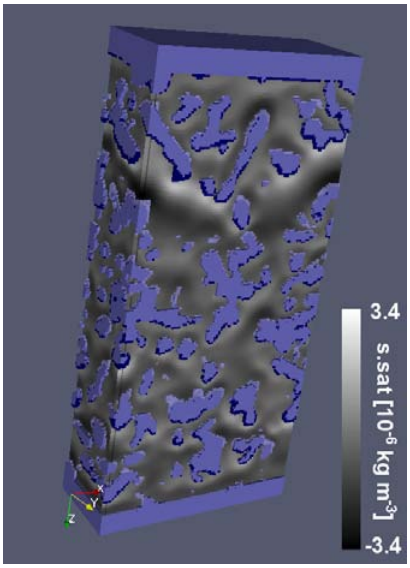


Figure 6: Simulation of metamorphism of sample 1. The sublimated (light blue) and condensed (dark blue) ice during one day and the supersaturation field (gray) at the end of the simulation (domain size 1.0×2.5×5.2 mm).

## 4. HEAT- AND MASS TRANSPORT

The $\mu$-CT experiments together with the numerical simulation represent a unique tool to investigate heat and mass fluxes within metamorphosing snow as well at the local, grain-size scale as at the global scale of the whole sample.

### *4. Local fluxes*

Using the numerical simulations, we can determine the heat and mass flows within the ice matrix and in the pore space (Fig. 7). We observe that the heat flow concentrates along the ice-matrix, the higher conducting material. Very high differences in heat flow are predicted locally, that is, on the grain scale. This leads to a highly inhomogeneous temperature field in the pore space, inducing itself inhomogeneous water vapor concentration gradients and flows. Note that the regions of high water vapor gradients coincide with high sublimation and grain growth rates at adjacent crystal interfaces (Fig. 6).

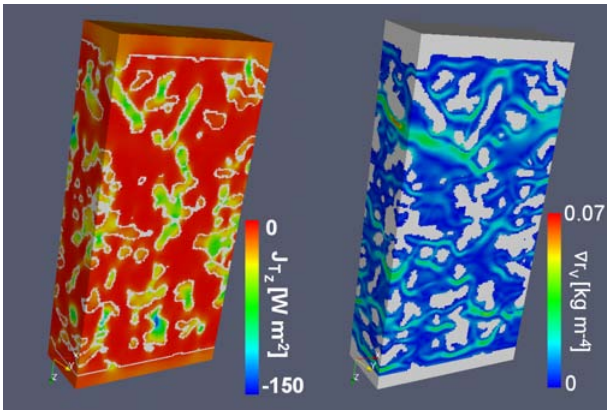


Figure 7: Computed heat flow in *z* (left) and norm of water vapor density gradient (right) after one day in sample 1 (size 1.0×2.5×5.2 mm, *z* axis is top to bottom).

Experimentally, we could observe the growth of individual snow crystals in detail (Fig. 2). By isolating such crystals (Fig. 8) and measuring their dimensions, growth velocities can be computed. For the cup-crystal of sample 2, which develops from a hexagonal plate to a cup with c-axis length of 0.7 mm during 60 h, this leads to a growth velocity in this direction of $3.2 \cdot 10^{-9}$ m s$^{-1}$, which corresponds to a vapor flow ahead of the crystal surface and along this growth direction of $2.8 \cdot 10^{-6}$ kg m$^{-2}$ s$^{-1}$.

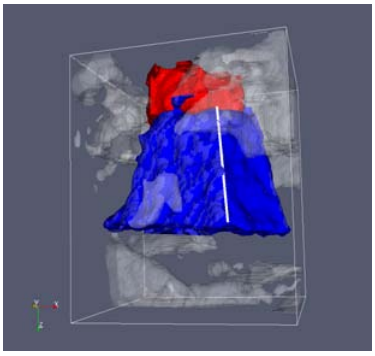

Figure 8: Hexagonal plate (red) growing to a cup-crystal (blue) during 60 h in sample 2. The white line is 0.7 mm in length.

### *4.2 Global fluxes*

We recur to a technique from particle image velocimetry (PIV) to experimentally determine the global mass flow through the snow sample. Using two successive $\mu$-CT images, a virtual movement of the ice-matrix is computed by comparing voxels region by region and determining the ideal displacement vectors (Fig. 9). But this virtual ice-matrix movement corresponds to an invisible water vapor transport through the pores. We can thus compute the water vapor flow though an *xy*-section by projecting the inverse vector field onto the z-axis and multiplying by the slice-density.

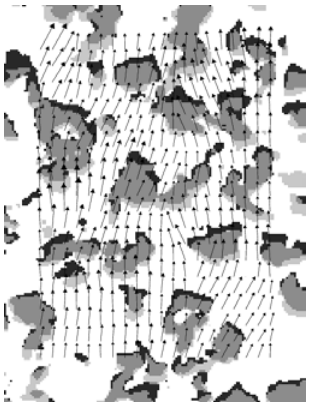

Figure 9: The inverse mass flow field determined by PIV on two successive $\mu$-CT images (2D slice of 3D calculation).

We computed mean water vapor flows on the order of $2 \cdot 10^{-7}$ and $4 \cdot 10^{-7}$ kg m$^{-2}$ s$^{-1}$ for samples 1 and 2. While the results fluctuated during the experiments by $\pm 1 \cdot 10^{-7}$ kg m$^{-2}$ s$^{-1}$ for both samples, no trend of increase or decrease in the mass flow

during metamorphism was observed. Note also that the flow rates are on the order of but lower than free water vapor diffusion through saturated air at equivalent temperatures and gradients. This is consistent with the work by Giddings and LaChapelle (1962) on depth-hoar growth.

The water vapor flow also contributes to the heat transport through the snow by latent heat. However, the measured mass flow rates would correspond to a heat transport on the order of 0.5 to 1 W $m^{-2}$, while the measured total heat flow through the snow samples determined by the heat flow plates in the snow breeder was on the order of 15 W $m^{-2}$.

From the measured heat flow we determined an effective heat conductivity of the snow by relating the measured flux to the imposed temperature gradient (Fig. 10). We observed a general trend of increasing heat conductivity during TG metamorphism, in contrast to the water vapor flow.

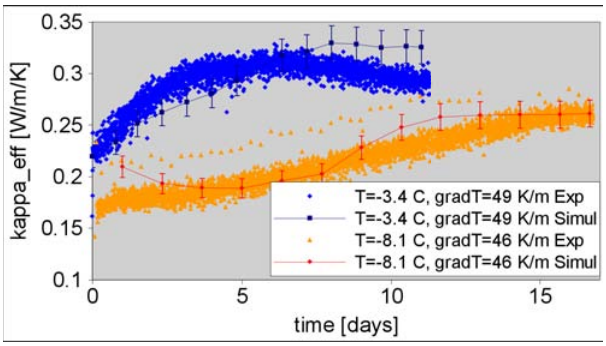


Figure 10: Measured and computed heat conductivity through the metamorphosing snow.

We also determined the effective heat conductivity of the snow samples numerically (Fig. 10). Since from the measurements we conclude that latent heat transport can be neglected in our two cases, we performed steady state heat diffusion simulations on the series of experimental $\mu$-CT images. Note that the sole input parameters to the numerical model were the heat conductivities of the ice and air, and the micro-structure of the snow through the $\mu$-CT scan. As well the increasing trend as the order of magnitude of the results correspond very well with the experiments.

## 5. CONCLUSION

We used $\mu$-CT imaging together with a micro-structural numerical model to study temperature gradient snow metamorphism. The experiments allow for a detailed observation of the structural changes, including grain growth within the snow pack. Moreover, global heat and mass flow rates through the snow can be determined.

Using the numerical model we showed that strong inhomogeneities of heat and mass flows must exist at the micro-structural (grain size) scale. As a step towards model validation we compared measured and computed effective heat conductivities through the snow and the results agree very well.

While grain growth rates can be significantly larger than global mass flow through the metamorphosing snow, we did not observe any global water vapor flux enhancement and the fluxes seemed to remain constant throughout the experiments. This is in contrast to the increasing heat conductivities that we observed and simulated for our snow samples.

Our approach shows the potential of an integral experimental-numerical approach that operates at the micro-structural length-scale and considers snow as a complex and metamorphosing porous material.

## ACKNOWLEDGMENTS

We thank Mathis Plapp from Ecole Polytechnique, Palaiseau, France, for his input on the numerical model. This project was funded by the Army Basic Research Terrain Properties and Processes Program and the Swiss National Science Foundation grant 200021-100294/1 and 200021-108219/1. It has been supported in part by an appointment to the Research Participation Program at the USACRREL administered by the Oak Ridge Institute for Science and Education through an interagency agreement between the U.S. Department of Energy and USACRREL.

## REFERENCES

Arons E. M. and S. Colbeck, 1995. Geometry of heat and mass transfer in dry snow: A review of theory and experiment. Rev. Geophys. 33(4), 463-493.

Boettinger W. J., J. A. Warren, C. Beckermann, and A. Karma, 2002. Phase-field simulations of solidification. Ann. Rev. Mater. Res. 32, 163-194.

Brzoska J.-B., C. Coléou, B. Lesaffre, S. Borel, O. Brissaud, W. Ludwig, E. Boller, and J. Baruchel, 1999. 3D visualization of snow samples by microtomography at low temperature. European Synchrotron Radiation Facility Newsletter 32, 22-23.

Christon M., P. J. Burns, and R. A. Sommerfeld, 1994. Quasi-steady temperature gradient metamorphism in idealized, dry snow. Numer. Heat Transfer. 25(A), 259-278.

Flin F., J.-B. Brzoska, B. Lesaffre, C. Coléou, and R. A. Pieritz, 2003. Full three-dimensional modelling of curvature-dependent snow metamorphism: First results and comparison with experimental tomographic data. J. Phys. D: Appl. Phys. 36(10A), A4-A54.

Giddings J. C. and E. LaChapelle, 1962. The formation rate of depth hoar. J. Geophys. Res. 67(6), 2377-2383.

Kaempfer Th. U., M. Schneebeli, and S. A. Sokratov, 2005. A microstructural approach to model heat transfer in snow. Geophys. Res. Lett. 32, L21503.

Kaempfer Th. U. and M. Plapp, 2007. Modeling heat and mass transfer in snow at a microstructural level using a phase-field approach – First results. Proceedings of the 64th Eastern Snow Conference, 173-177.

Kaempfer Th. U. and M. Plapp, 2008. Phase-field modeling of dry snow metamorphism, Phys. Rev. E, submitted

Kerbrat M., B. Pinzer, T. Huthwelker, H. W. Gaggeler, M. Ammann, and M. Schneebeli, 2008. Measuring the specific surface area of snow with X-ray tomography and gas adsorption: comparison and implications for surface smoothness. Atmos. Chem. Phys. 8(5), 1261-1275

Schneebeli M., and S. A. Sokratov, 2004. Tomography of temperature gradient metamorphism of snow and associated changes in heat conductivity. Hydrol. Process. 18(18), 3655-3665.